Free volume from positron lifetime and pressure–volume–temperature experiments in relation to structural relaxation of van der Waals molecular glass-forming liquids

2010 J. Phys.: Condens. Matter 22 235104

(http://iopscience.iop.org/0953-8984/22/23/235104)

IOP Publishing Journal of Physics: Condensed Matter

J. Phys.: Condens. Matter **22** (2010) 235104 (10pp) doi:10.1088/0953-8984/22/23/235104

Free volume from positron lifetime and pressure–volume–temperature experiments in relation to structural relaxation of van der Waals molecular glass-forming liquids

G Dlubek[1,4], M Q Shaikh[2], K Rätzke[2], M Paluch[3] and F Faupel[2]

[1] ITA Institute for Innovative Technologies, Köthen/Halle, Wiesenring 4, D-06120 Lieskau, Germany
[2] Faculty of Engineering, Institute for Materials Science, Christian-Albrechts University of Kiel, Kaiserstraße 2, D-24143 Kiel, Germany
[3] Institute of Physics, Silesian University, Uniwersytecka 4, 40-007 Katowice, Poland

E-mail: guenter.dlubek@gmx.de

Received 28 January 2010, in final form 14 April 2010
Published 26 May 2010
Online at stacks.iop.org/JPhysCM/22/235104

Abstract

Positron annihilation lifetime spectroscopy (PALS) is employed to characterize the temperature dependence of the free volume in two van der Waals liquids: 1,1′-bis(*p*-methoxyphenyl)cyclohexane (BMPC) and 1,1′-di(4-methoxy-5-methylphenyl)cyclohexane (BMMPC). From the PALS spectra analysed with the routine LifeTime9.0, the size (volume) distribution of local free volumes (subnanometer size holes), its mean, $\langle v_h \rangle$, and mean dispersion, σ_h, were calculated. A comparison with the macroscopic volume from pressure–volume–temperature (PVT) experiments delivered the hole density and the specific hole free volume and a complete characterization of the free volume microstructure in that sense. These data are used in correlation with structural (α) relaxation data from broad-band dielectric spectroscopy (BDS) in terms of the Cohen–Grest and Cohen–Turnbull free volume models. An extension of the latter model allows us to quantify deviations between experiments and theory and an attempt to systematize these in terms of T_g or of the fragility. The experimental data for several fragile and less fragile glass formers are involved in the final discussion. It was concluded that, for large differences in the fragility of different glass formers, the positron lifetime mirrors clearly the different character of these materials. For small differences in the fragility, additional properties like the character of bonds and chemical structure of the material may affect size, distribution and thermal behaviour of the free volume.

1. Introduction

As the temperature of a glass-forming liquid is reduced, the molecular motions become more restricted, due to both the decrease of thermal energy and the increase of molecular crowding. Therefore, one important and common feature of the dynamics of glass-forming liquids is the relation between the molecular mobility and the microstructure and amount of free volume. Although very important, this aspect still provokes controversy when different interpretations are discussed [1–5].

Positron annihilation lifetime spectroscopy (PALS) is known to be a very powerful experimental method for studying the free volume in crystals, glasses and liquids [6, 7]. In PALS, positronium in its ortho-state (spin 1), *o*-Ps, is used as a probe for subnanometer size local free volumes (holes). Ps forms in the terminal spur (blob) of the fast positron

[4] Author to whom any correspondence should be addressed.

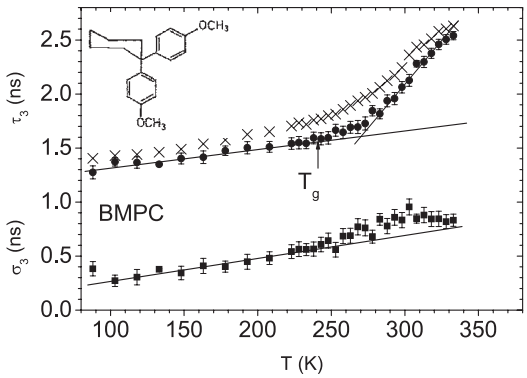

Figure 1. Mean, $\tau_3 \equiv \langle\tau_3\rangle$ and standard deviation, σ_3, of the *o*-Ps lifetime distribution of BMPC (filled symbols). The lines through the data points (filled symbols) are a visual aid, T_g shows the glass transition from BDS [8]. For comparison, the parameters from the unconstrained discrete term fit are shown by crosses.

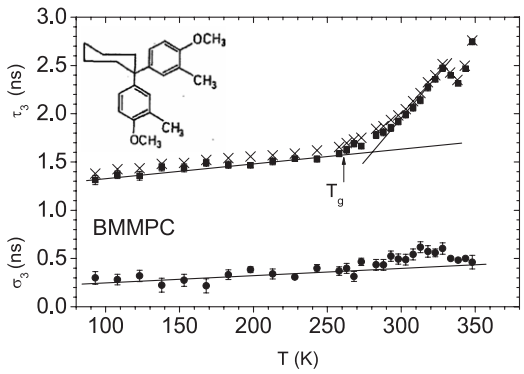

Figure 2. As for figure 1, but BMMPC. T_g from BDS [9].

track from a decelerated positron and one of the knocked-out thermalized track electrons. It becomes (Anderson) localized in a local free volume (hole) and annihilates via pick-off with an electron other than its own bound partner and with opposite spin during collisions with molecules in the hole wall. This reduces the *o*-Ps' lifetime from its value in a vacuum, 142 ns (self-annihilation), to the low nanosecond range (pick-off annihilation).

In this work, with the help of PALS we study the free volume of two van der Waals liquids: 1,1′-bis(*p*-methoxyphenyl)cyclohexane (BMPC) and 1,1′-di(4-methoxy-5-methylphenyl)cyclohexane (BMMPC) and relate this to the structural relaxation data as measured previously by one of us by broad-band dielectric relaxation spectroscopy (BDS) [5, 8, 9]. The chemical structure of the molecules are shown in the inset of figures 1 and 2. The aim of our study is to characterize the free volume as completely as possible and to use this to test the validity of the Cohen–Turnbull [1] and Cohen–Grest [2] free volume theories, to discover possible deviations from the expected behaviour, and to discuss physical reasons for these deviations. Low molecular-weight organic glass formers have already been studied by several groups and the PALS data were correlated to viscosity, dielectric relaxation and incoherent elastic neutron scattering measurements [10–15]. As for our previous projects on phenylphthalein dimethylether (PDE) [16], phenyl salicylate (Salol) [17] and Verapamil hydrochloride [18] we go beyond these former works by measuring the positron lifetime spectra with a high statistical accuracy and analysing the distribution of lifetimes utilizing the routine LifeTime, version 9.0 (LT9.0) [19]. From the *o*-Ps lifetime distribution we calculate the hole size distribution and characterize this by its mean and width. The lifetime distributions, although hard to determine precisely, contain more information than can be obtained from the conventional mean lifetime and mean hole size approach (discrete exponential lifetime analysis). Furthermore, we estimate the hole density and the specific hole free volume from a correlation of PALS with pressure–volume–temperature (PVT) experiments (from [5]) as performed recently for polymers [20, 21] and small-molecule liquids [16–18].

2. Experiments

The BMPC and BMMPC samples for PALS measurements were prepared from the same materials as investigated in the past by broad-band dielectric spectroscopy (BDS) [8, 9, 22, 23] and pressure–volume–temperature (PVT) experiments [5]. The chemical structure of the materials is shown in the inset of figures 1 and 2. They were synthesized in the laboratory of Professor Sillescu at Johannes Gutenberg University, Mainz, Germany. The samples were delivered as crystalline powders and have a melting temperature of 331 K (BMPC) and 346 K (BMMPC). The glass transition temperatures T_g determined from BDS experiments assuming a primary (α) relaxation time of 10^2 s are 241 K and 261 K, respectively.

Positron annihilation lifetime experiments have been performed with a fast–fast coincidence set-up [7] using a home-made temperature-controllable sample holder under high vacuum conditions. The time resolution was 285 ps (FWHM, ^{22}Na source) and the analyser channel width amounted to 25.3 ps. The materials available in the form of crystalline powder were sandwiched around a ∼1 MBq positron source: ^{22}NaCl, deposited between two 7 μm thick kapton foils. They were heated in the sample holder to T_m+5 K for melting and measured at this temperature. Subsequently, the sample was cooled to 93 K and the temperature run was started. This treatment supercools the melt and transforms the samples at low temperatures into an amorphous, glassy state. During the experiments the temperature was increased between 103 K and $T_m + 5$ K in steps of 15 K below 223 K and 5 K above that temperature, respectively (accuracy of ±2 K). Source correction, 8.4% of 395 ps (kapton foil and ^{22}NaCl), and time resolution were determined by measuring a defect-free p-type silicon reference ($\tau = 219$ ps). The final resolution function used in the spectrum analysis was determined as a sum of two Gaussian curves. Each measurement lasted 2 h, leading to a lifetime spectrum with the high number of $\sim 5 \times 10^6$ annihilation events, which is sufficiently high to be analysed with the routine LT9.0 in its distribution mode.

3. Results and discussion

3.1. Spectrum analysis and lifetime parameters

The (ideal) positron lifetime spectrum $s(t)$ is given by the Laplace transformation of the sum of the functions $\alpha_i(\lambda)\lambda$, $s(t) = \sum I_i \int \alpha_i(\lambda)\lambda \exp(-\lambda t)\,\mathrm{d}\lambda$, where $\alpha_i(\lambda)$ is the distribution (probability density function, pdf) of the annihilation rate $\lambda = 1/\tau$ of the decay channel i [7]. The routine LifeTime version 9.0 (LT9) [19] describes the $\alpha_i(\lambda)$ by log-normal functions where the finite width of the distribution comes from the size (and shape) distribution of holes which are related to thermal fluctuations [24–26]. The positron decay in molecular amorphous solids and in liquids usually shows three decay channels which are attributed to the annihilation of p-Ps (τ_1), free (not Ps) positrons (e^+, τ_2) and o-Ps (τ_3; $\tau_1 < \tau_2 < \tau_3$, $\sum I_i = 1$) [7]. For reducing the number of fitting parameters we assumed the short p-Ps and e^+ lifetimes appear discrete ($\sigma_1 = \sigma_2 = 0$) while the large o-Ps shows a distribution with the standard deviation $\sigma_3 > 0$. These assumptions lead to stable fits with reduced chi-squares of $\chi^2/df < 1.06$.

Figures 1 and 2 show the most important results, the mean $\tau_3 \equiv \langle\tau_3\rangle$ ($\langle\tau_i\rangle = \int \tau\alpha_i(\tau)\,\mathrm{d}\tau$, $\int \alpha_i(\tau)\,\mathrm{d}\tau = 1$), and the mean dispersion σ_3 (square root of the variance $\sigma_i^2 = \int(\tau - \langle\tau_i\rangle)^2\alpha_i(\tau)\,\mathrm{d}\tau$) of the o-Ps lifetime distribution $\alpha_3(\tau) = \alpha_3(\lambda)\lambda^2$. τ_3 varies between 1.3 and 2.7 ns and shows a typical glass transition behaviour, with a distinct increase in its slope at T_g, which is closely followed by σ_3 with the ratio $\sigma_3/(\tau_3 - 0.5) \approx 0.5$ (BMPC) and ≈0.3 (BMPC) (0.5 ns is the lowest possible lifetime of o-Ps for vanishing hole size, see below). For comparison with the literature, the figures show also the lifetime τ_3 obtained from discrete term fits $\sigma_1 = \sigma_2 = \sigma_3 = 0$. These fitted values appear larger than those from the distribution analysis: the broader the o-Ps lifetime distribution (σ_3), the larger these values are. The intensity of the o-Ps component (not shown) for both samples increases slightly with T from 10% to 13%.

The lifetime of positrons e^+ (not bound into Ps), τ_2 (not shown), varies parallel to τ_3 between 0.31 and 0.36 ns (BMPC) and 0.28 and 0.33 ns (BMMPC). A plot of τ_2 versus τ_3 (all lifetimes in nanoseconds) can be described by the linear relation (all lifetimes in nanoseconds)

$$\tau_2 = A + B(\tau_3 - 0.5). \tag{1}$$

From linear fits we obtained $A = (0.275 \pm 0.004)$ ns and $B = (0.038 \pm 0.003)$ for BMPC, and $A = (0.274 \pm 0.005)$ ns and $B = (0.024 \pm 0.004)$ for BMMPC. The temperature dependence of τ_2 mirrors the size of the local empty spaces in which positrons (e^+) annihilate. The fitting parameter A in equation (1) may be considered as a measure of the bulk lifetime of positrons in the corresponding material while B describes the influence of the free volume size on τ_2. For Verapamil hydrochloride [18], for example, we analysed values of $A = (0.288 \pm 0.001)$ ns and $B = (0.0376 \pm 0.001)$. The p-Ps lifetime (not shown) varies statistically between 0.14 and 0.17 ns with a mean of $\tau_1 = (0.155 \pm 0.01)$ ns for BMPC and $\tau_1 = (0.145 \pm 0.01)$ ns for BMMPC.

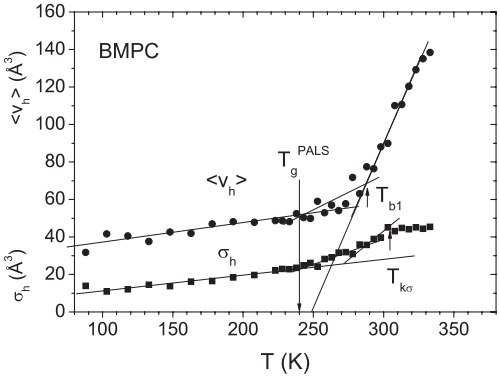

Figure 3. The mean, $\langle v_h\rangle$, and the standard deviation, σ_h, of the hole volume distribution $g_n(v_h)$ as a function of the temperature T for BMPC. The straight lines through the data points (filled symbols) are a visual aid. For the characteristic temperatures see the text.

3.2. Temperature dependence of the hole size

In the following section we have calculated the hole volume distribution from the o-Ps annihilation rate distribution and discuss the temperature dependence of the mean and width of this distribution. Based on the semi-empirical standard model [27] the o-Ps pick-off annihilation rate λ_{po}, the inverse of the o-Ps lifetime $\tau_{po} = \tau_3$, is related to the hole (assumed spherical) radius (r_h) via

$$\lambda_{po} = 1/\tau_{po} = 2\ \mathrm{ns}^{-1}\left[1 - \frac{r_h}{r_h + \delta r} + \frac{1}{2\pi}\sin\left(\frac{2\pi r_h}{r_h + \delta r}\right)\right], \tag{2}$$

where the parameter $\delta r = 1.66$ Å [27, 28] describes the penetration of the Ps wavefunction into the hole walls. The mean hole volume is usually calculated from $v_h(\tau_3) = (4/3)\pi r_h^3(\tau_3)$. Since λ_{po} follows a distribution, we have estimated, as in our previous works [16–18, 24–26], the mean hole volume as the mass centre of the hole size distribution. The radius distribution, $n(r_h)$, can be calculated from $n(r_h) = -\alpha_3(\lambda)\,\mathrm{d}\lambda/\mathrm{d}r_h$, where $\alpha_3(\lambda)$ is the o-Ps annihilation rate distribution calculated from the parameters of the LT analysis. The hole volume distribution follows from $g(v_h) = n(r_h)/4\pi r_h^2$ and is considered as a volume-weighted function. The number-weighted hole size distribution follows then from $g_n(v_h) = g(v_h)/v_h$. We have calculated the mean $\langle v_h\rangle$ and the variance σ_h^2 of $g_n(v_h)$ as the first and second moments of this distribution.

Figures 3 and 4 show these parameters for our samples. Below T_g the mean hole volume shows a flat, linear rise with an increase in the slope above the glass transition. For BMPC, and more pronounced for BMMPC, the transition at T_g from the small slope to the large slope region is rather smooth. Following the concept of Bartoš *et al* [10–13] the temperature dependence of $\langle v_h\rangle$ (or τ_3) may be subdivided into four linear parts: a very flat increase below T_g, a medium increase between T_g and T_{b1}, a strong increase between T_{b1} and T_{b2} (denoted by us as T_k, see below) and a flat behaviour above that temperature (compare figure 3). These authors found some coincidences of T_{b1} with changes in the properties of the secondary (β) relaxation process in different glass formers [12, 13]. From the

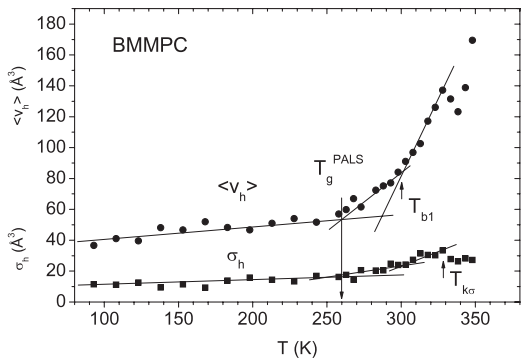

Figure 4. As for figure 3 but BMMPC.

Table 1. Results from the analysis of the PALS and PVT experiments (for an explanation of symbols see text).

Quantity	Uncertainty	BMPC	BMMPC
T_g^{PALS} (K)	±5	240	260
T_{b1} (K)	±3	290	300
$\langle v_{hg}\rangle$ (Å^3)	±3	52	51
σ_{hg} (Å^3)	±3	22	19
e_{hg} (Å^3 K^{-1})[a]	±0.02	0.10	0.11
e_{hr} (Å^3 K^{-1})[b]	±0.07	1.55	1.82
V (300 K) (cm^3 g^{-1})	±0.0002	0.928	0.926
V_{occ} (cm^3 g^{-1})[c]	±0.003	0.8873	0.8950
N'_h (10^{21} g^{-1})[c]	±0.04	0.45	0.36
N_h (300 K) (nm^{-3})	±0.05	0.48	0.39
$E_{fg} = dV_f/dT$ (10^{-4} cm^3 K^{-1})[a]	±0.06	0.37	0.36
$E_{fr} = dV_f/dT$ (10^{-4} cm^3 K^{-1})[c]	±0.3	7.4	6.1

[a] At $T \to T_g$, $T < T_g$. [b] For T = 293–233 K (BMPC) and T = 303–323 K (BMMPC). [c] For T = 310–343 K (BMPC) and T = 303–353 K (BMMPC).

data plotted in figures 3 and 4 we estimate $T_{b1} = (290 \pm 3)$ K (BMPC) and (300 ± 3) K (BMMPC), respectively. Table 1 shows the values of mean hole volume $\langle v_{hg}\rangle$ and its mean dispersion σ_{hg} at T_g and the corresponding slopes in the mean hole volume (thermal expansivities $e_h = d\langle v_h\rangle/dT$) for different temperature ranges (g—glass, $T < T_g$; r—rubber, $T > T_{b1}$).

At a higher temperature T_{kv} (the 'knee' temperature, in some articles in the literature, marked by T_e, T_{b2} or T_r) the increase of $\langle v_h\rangle$ shows usually a tendency to level off. The T_{kv} is not clearly detected in our experiments for BMPC and BMMPC but is expected to appear somewhat above the highest temperature of the experiment (see the discussion below and figure 10). We have attributed this well-known behaviour to an artefact coming from the movement of hole walls during the life of o-Ps [16–18, 24–26]. At temperatures below T_{kv} the structural relaxations are slow and the o-Ps probe makes snapshots from the free volume structure which fluctuates in space and time. This leads to the observed distribution of o-Ps lifetimes. Above T_{kv} this is not true any more and $\langle v_h\rangle$ (τ_3) levels off. We remark that some different mechanisms such as 'cage rattling' [15] and Ps-bubble formation [29] were also discussed in the literature. The width σ_h of the hole volume distribution behaves almost parallel to $\langle v_h\rangle$, but shows

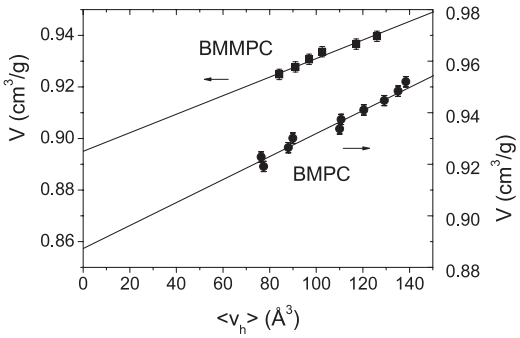

Figure 5. Plot of the specific volume $V(T)$ of BMPC and BMMPC versus the mean hole volume $\langle v_h(T)\rangle$ for zero pressure. The lines are linear fits to the data from the temperature range between 293 K ($> T_{b1}$) and 333 K (BMPC) and between T_{b1} = 303 K and 323 K (BMMPC), respectively.

its 'knee' at lower temperatures $T_{k\sigma} < T_{kv}$. Based on a fluctuation approach the knee at $T_{k\sigma}$ has been attributed by some of us to the disappearance of the dynamic heterogeneity (for details see [24, 26]).

3.3. The hole density calculated from the specific total and the free volume

To estimate the hole density we need to know the temperature dependence of the macroscopic volume V. PVT experiments in the pressure range up to 200 MPa and in the temperature range between 310 K and 341 K (BMPC) and 303 K and 353 K (BMMPC), respectively, were published by one of us previously (figures 1 and 2 of [5]). We reanalysed these data here by fitting them to the empirical Tait equation [30]:

$$V(P,T) = V(0,T)\{1 - C\ln[1 + P/B(T)]\} \qquad (3)$$

with $V(0,T) = \sum C_n T^n$ (n = 0, 1, 2) and $B(T) = B_0 \exp(-B_1 T)$. Here V is given in cm^3 g^{-1} and T, as usual for this kind of analysis, in degrees Celsius. A fixed value of $C = 0.0894$ has been customarily used, following the original analysis of hydrocarbons. This analysis was also applied in [5]. For getting better fits we allowed C to vary here and got from the simultaneous least-squares fits to the parameters shown in table 2 ($R^2 = 0.9998$). The analysed parameters correspond closely to those from the previous work except the value of C_0 where a mistake appeared in [5].

For the estimation of the number density of holes we use the empirical relation [20, 21, 24, 25]

$$V = V_{occ} + N'_h\langle v_h\rangle, \qquad (4)$$

where V, V_{occ} and $V_f = N'_h\langle v_h\rangle$ are the specific total, occupied and free volumes, respectively, and N'_h is the mean specific hole density. Our previous works, as well as results of other groups on polymers, have proved that in the temperature range above T_g, V_{occ} and N'_h are constant. This appears to be true also for low molecular-weight glass formers [16–18]. Reasons for this behaviour were discussed in detail in previous works [31, 32].

For the estimation of N'_h we have plotted in figure 5 the specific volume $V(T)$ calculated from the parameters of

Table 2. Results from the Tait analysis of PVT experiments.

	C_0 ($cm^3\ g^{-1}$)	C_1 ($10^{-4}\ cm^3\ g^{-1}\ C^{-1}$)	C_2 ($10^{-7}\ cm^3\ g^{-1}\ C^{-2}$)	C	B_0 (MPa)	B_1 ($10^{-3}\ C^{-1}$)
BMPC	0.908 43 ±0.000 2	7.3 ±0.02	0	0.0709 ±0.0004	203.5 ±2	4.55 ±0.1
BMMPC	0.910 76 ±0.000 2	5.6 ±0.06	4.192 ±0.5	0.0682 ±0.0004	238.9 ±2	5.24 ±0.1

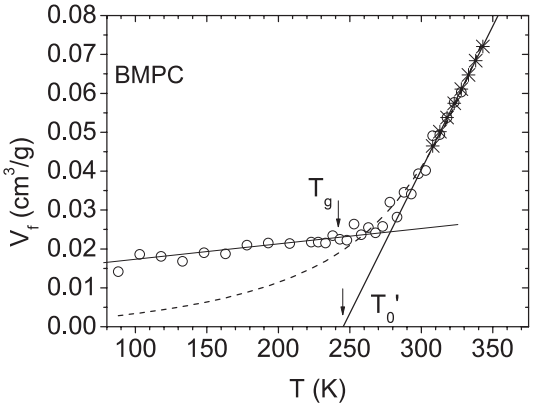

Figure 6. Specific free volume calculated from PALS, $V_f = N_h'\langle v_h\rangle$ (open circles), and PVT data, $V_f = V - V_{occ}$ (stars), for BMPC. The lines show the following fits: solid—linear fit to V_f in the temperature range 303–343 K; dashed—fit of the CG equation with free variable $T_0'^{CG}$ (=328 ± 25 K) in the range above 245 K.

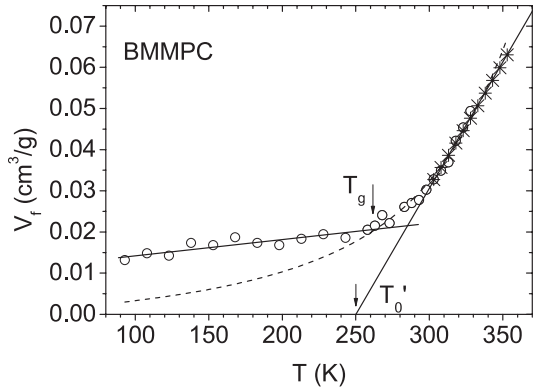

Figure 7. Specific free volume calculated from PALS, $V_f = N_h'\langle v_h\rangle$ (open circles), and PVT data, $V_f = V - V_{occ}$ (stars), for BMMPC. The lines show the following fits: solid—linear fit to V_f in the temperature range between 310 and 353 K; dashed—fit of the CG equation with free variable $T_0'^{CG}$ (=365 ± 25 K) in the range above 263 K.

the Tait equation versus the o-Ps hole volume $\langle v_h(T)\rangle$ in the temperature range above T_{b1}. A linear fit to the data of BMPC gives the parameters $V_{occ} = (0.8873 \pm 0.005)\ cm^3\ g^{-1}$ and $N_h' = dV/d\langle v_h\rangle = (dV/dT)/(d\langle v_h\rangle/dT) = (0.45 \pm 0.04) \times 10^{-21}\ g^{-1}$. For BMMPC we obtained $V_{occ} = (0.8950 \pm 0.005)\ cm^3\ g^{-1}$ and $N_h' = (0.36 \pm 0.04) \times 10^{-21}\ g^{-1}$. The specific hole densities correspond at 300 K to volume-related hole densities of $N_h = N_h'/V = 0.48\ nm^{-3}$ and $0.39\ nm^{-3}$, respectively (see table 1). The hole density determined here corresponds to that estimated for other low molecular-weight glass formers ($0.44\ nm^{-3}$ for PDE [16] and $0.75\ nm^{-3}$ for Salol [17]).

These results now allows us to calculate the specific hole free volume either from PALS, $V_f = N_h'\langle v_h\rangle$ (including low temperatures by the assumption that N_h' stays constant also here), or from PVT data, $V_f = V - V_{occ}$ (above room temperature). These data are displayed in figures 6 and 7. At T_g we obtain $V_f(T_g) = V_{fg} = 0.022\ cm^3\ g^{-1}$ for BMPC and $V_{fg} = 0.021\ cm^3\ g^{-1}$ for BMMPC. The total variation of V_f ranges from ∼0.015 at 100 K to 0.07–0.08 at 350 K.

The specific free volume V_f shows at higher temperatures a linear behaviour. Therefore, we have fitted the PALS and PVT data from the temperature range above 300 K by the function

$$V_f = E_f(T - T_0'), \tag{5}$$

where E_f is the specific thermal expansivity and T_0' the temperature where the linearly extrapolated specific free volume vanishes (compare figures 6 and 7). Table 1 shows the fitted parameters (E_{fr}, T_0') together with expansivity of the glass, E_{fg}.

As a second possibility we describe the free volume data by the Cohen–Grest (CG) free volume model [2]. The CG model divides the system into liquid-like and solid-like cells; only the former have free volumes large enough to be suitable for structural movements. Cohen and Grest derived that the free volume varies as

$$V_f(T) = B'^{CG}\{T - T_0'^{CG} + [(T - T_0'^{CG})^2 + C'^{CG}T]^{1/2}\}, \tag{6}$$

(for the meaning of the constants see [2]). $T_0'^{CG}$ is identified as the temperature at which continuity of the liquid-like molecules is attained (percolation threshold). A fit to the PALS and PVT data of BMPC from the temperature range between 245 and 350 K delivered $T_0'^{CG} = 328(\pm 25)$ K ($R^2 = 0.984$, table 3). As figure 6 shows, the fit describes well the flat transition of the free volume above T_g from a small to the larger slope without the need to subdivide this temperature range into the segments $T < T_{b1}$ and $T > T_{b1}$. Due to the large statistical scatter of free volume data the fitted parameters show a large statistical error. As shown by Paluch *et al* [33] the primary relaxation data from BDS for BMPC, BMMPC and other glass formers like PDE and Salol can be excellently described over the whole range of experimental available temperatures by the CG free volume model. The characteristic temperature describing the thermal behaviour of the α relaxation, T_0^{CG}, was determined from these fits to be 288 K for BMPC and

Table 3. Fitted parameters from VFT plots ($\log_{10}\omega$ versus $1/T$), CT plots ($\log_{10}\omega$ versus $1/V_f$) and CG plot (ω or V_f versus T). For the meaning of parameters see the text.

(a) BDS		Salol	BMPC	BMMPC	PDE	VH
T_g ($\tau_\alpha = 100$ s) (K)		220 ± 2	241 ± 2	261 ± 2	294 ± 2	320 ± 2
T_0^{CG} (K [10])	$T > T_g$	249 ± 2	288 ± 2	314 ± 2	320 ± 2	309 ± 5
T_B (K)		265 ± 3	275 ± 3	330 ± 3	325 ± 3	—
T_B/T_g^{BDS}		1.20	1.14	1.26	1.11	—
T range of fit (K)	$T < T_B$	220–245	242–270	260–325	295–315	
	$T > T_B$	265–420	275–380	335–395	325–420	320–380
$\log_{10}[\omega_0$ (rad s^{-1})]	$T < T_B$	20.4 ± 0.6	29.5 ± 0.2	20.4 ± 0.2	29.4 ± 0.7	
	$T > T_B$	11.2 ± 0.1	14.2 ± 0.13	11.20 ± 0.1	11.1 ± 0.1	15.01 ± 0.1
B (K^{-1})	$T < T_B$	3185 ± 200	8328 ± 500	4854 ± 90	8838 ± 460	
	$T > T_B$	343 ± 8	1156 ± 40	484 ± 12	53 ± 20	2430 ± 53
T_0 (K)	$T < T_B$	158.2 ± 3	126 ± 4	166.8 ± 1	171.4 ± 3.5	
	$T > T_B$	224 ± 2	218.8 ± 1	276.7 ± 1	278 ± 2	258.04 ± 1
m ($T \to T_g$)	$T < T_B$	80	66	62	75	87
(b) PALS/PVT		Salol	BMPC	BMMPC	PDE	VH
T_g^{PALS} (K)		220 ± 5	240 ± 5	260 ± 5	285 ± 5	294 ± 5
$T_0'^{CG}$ (K)	$T > T_g$	216 ± 5	328 ± 25	365 ± 25	279 ± 10	312 ± 15
$T_{k\tau 3}/T_g^{PALS}$		1.23	$\approx$1.38	$\geqslant$1.26	1.21	1.35
T_0' (K)	$T > T_{b1}$	170 ± 5	246 ± 5	250 ± 5	253 ± 3	237 ± 10
$\log_{10}[C$(rad s^{-1})]	$T < T_B$	25.4 ± 0.4	n.d.	n.d.	25.4 ± 0.6	
	$T > T_B$	11.1 ± 0.1	11.8 ± 0.04	10.9 ± 0.1	11.80 ± 0.1	15.01 ± 0.1
γV_f^* (cm^3 g^{-1})	$T < T_B$	2.74 ± 0.09	n.d.	n.d.	2.86 ± 0.13	
	$T > T_B$	0.18 ± 0.01	0.246 ± 0.01	0.259 ± 0.01	0.313 ± 0.01	1.24 ± 0.03
ΔV (10^{-2} cm^3 g^{-1})	$T < T_B$	-1.00 ± 0.1	n.d.	n.d.	0.024 ± 0.01	
	$T > T_B$	3.65 ± 0.3	1.26 ± 0.02	1.69 ± 0.04	1.38 ± 0.1	1.07 ± 0.05
E_f (10^{-4} cm^3 g^{-1} K^{-1})	$T > T_B$	6.3 ± 0.3	7.4 ± 0.3	6.1 ± 0.3	5.0 ± 0.5	5.09 ± 0.13
$T_0 - T_0'$ (K)	$T > T_B$	54	-27	27	25	21
ΔV_{calc} (10^{-2} cm^3 g^{-1})	$T > T_B$	3.4 ± 0.1	-2.0 ± 0.1	1.65 ± 0.1	1.25 ± 0.1	1.1 ± 0.1

314 K for BMMPC. As discussed here [33], T_0^{CG} agrees approximately with T_B, the temperature of the crossover from the VTF to another dynamics (see below). The temperatures given in table 3 at least roughly shows that such behaviour exists.

An attempt to fit the V_f data of BMPC with the CG model assuming $T_0'^{CG} = T_0^{CG} = 288$ K gives a somewhat less sufficient fit ($R^2 = 0.980$). The corresponding results for BMMPC are $T_0'^{CG} = 365(\pm 25)$ K ($R^2 = 0.9924$) (free fit). Again, a fit fixing $T_0'^{CG} = T_0^{CG} = 314$ K leads to a slightly more worse fit ($R^2 = 0.9895$). We may conclude from these results that the CG free volume model does not seem consistent to describe both relaxation and free volume data. This behaviour has been observed also for PDE, Salol and Verapamil hydrochloride [16–18]. We remark, however, again that the CG fit is only weakly sensitive to a variation of $T_0'^{CG}$ as large as 50 K. That is due to the high number of fitting parameters, the limited range of experimental free volume data (only those from above T_g can be used) and their large statistical scatter. We remark here also that the CG theory, while describing very excellently the temperature dependence of α relaxation at zero or ambient pressure, fails for systems under pressure [34]. It seems to be not clear whether this is due to the failure of the physical picture of the CG theory itself, or due to the way of extending the equation to the pressure dependence. It is assumed that T_0^{CG} and several other parameters change linearly with the pressure P. This may be an oversimplification. Further research including pressure-dependent PALS studies may help to solve this question.

3.4. Free volume and the primary (α) relaxation in terms of the Cohen–Turnbull free volume theory

The relaxation properties of glass formers and their physical backgrounds are still a matter of extensive discussions (see as examples [1–6, 35–39]). Here we focus on the primary (α) relaxation. The experimental data previously obtained from BDS [5, 8, 9] will be discussed in this section in terms of the classical free volume theory of mobility derived by Cohen and Turnbull [1] on the basis of the statistical mechanics. When applying this theory to the α relaxation, its mean frequency ω can be described in the temperature range $T > T_g$ by the well-known expression

$$\log_{10}\omega = \log_{10} C - (\gamma V_f^*/\ln 10)/V_f, \qquad (7)$$

where C is a pre-exponential factor, V_f is the mean specific (not fractional!) free volume of the liquid or rubbery material, γV_f^* is the minimum specific free volume required for the occurrence of the process and $\gamma = 0.5$–1.

The CT free volume theory has the advantage that it leads directly to the Vogel–Fulcher–Tammann (VFT) equation or its equivalent the Williams–Landel–Ferry (WLF) equation (see [36] and references given therein), both of which are commonly used to describe the temperature dependence of the structural relaxation in supercooled polymeric or small-molecule liquids. Assuming that the hole free volume expands

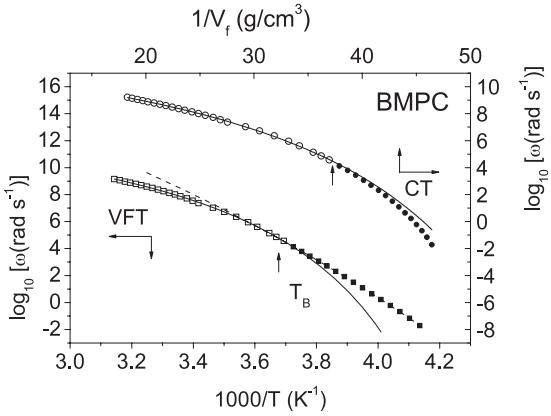

Figure 8. Arrhenius plot (VFT, squares, bottom x and left y axes) and Cohen–Turnbull plot (CT, circles, top x and right y axes) of the peak frequency $\omega = 2\pi f_{\max}$ of dielectric loss ε'' of the main relaxation process in BMPC. The frequency data are from [8] and cover a temperature range between 242 and 380 K. The lines show fits to the data in the temperature range between 275 and 380 K (open symbols, solid line, $T_B = 275$ K) and between 242 and 270 5 K (filled symbols, dashed line, only for VFT).

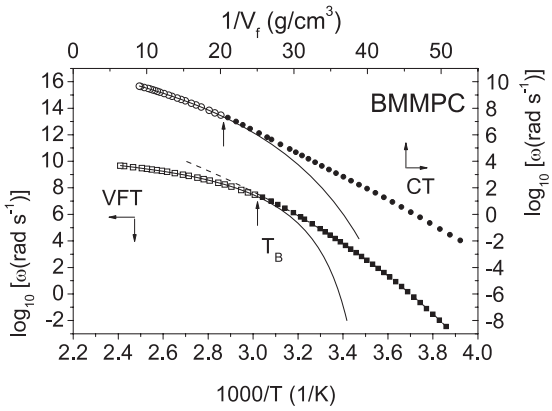

Figure 9. As for figure 8, but for BMMPC. The frequency data are from [9] and cover a temperature range between 260 and 395 K. The lines show fits to the data in the temperature range between 335 and 395 K (open symbols, solid line, $T_B = 330$ K) and between 260 and 325 K (filled symbols).

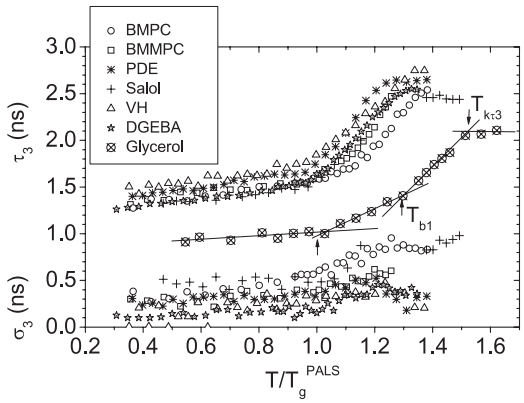

Figure 10. Mean, $\tau_3 \equiv \langle\tau_3\rangle$, and standard deviation, σ_3, of the o-Ps lifetime distribution of various small-molecule glass formers. The data for glycerol are from discrete term fits and no σ_3 value is available [10].

linearly, as is described by equation (5), formula (7) can be written in the form of the VFT equation

$$\log_{10}\omega = \log_{10}\omega_0 - (B/\ln 10)/(T - T_0), \qquad (8)$$

with $\omega_0 = C$, $T_0 = T_0'$ and $B = \gamma V_f^*/E_f$.

Figures 8 and 9, bottom parts, show a reproduction of the α relaxation data for BMPC and BMMPC from [8, 9]. Stickel plots (in the form $[\mathrm{d}\log\omega/\mathrm{d}T]^{-1/2} = (B/\ln 10)^{-1/2}(T - T_0)$ [39–41]) showed that the data from the whole temperature range do not follow a single VFT equation by splitting into two ranges separated by a transition temperature T_B. The data from the temperature range $T > T_B$ can be well fitted by the VFT equation. We have reanalysed the relaxation data and the fitting parameters, which shows close agreement with the results from the literature [8, 9, 41], tabulated in table 3 together with the results for PDE, Salol and Verapamil hydrochloride from our former works [16–18]. As discussed in the literature, the relaxation data from the temperature range $T_g < T < T_B$ frequently do not show a perfect VFT behaviour [41]. We, however, on a trial basis have also fitted these data by the VFT equation to get a complete set of parameters (table 3).

Analysis of the relaxation data of polymers and low-molecular-weight glass formers shows frequently that only a modification of equation (7) can be fitted to the experimental data. This equation is

$$\log_{10}\omega = \log_{10}C - (\gamma V_f^*/\ln 10)/(V_f - \Delta V), \qquad (9)$$

with ΔV being a volume correction term. Recently some of us [16–18, 24, 25, 42] proposed that $\Delta V > 0$ is an indication that it is not the entire specific hole free volume V_f, as calculated from PALS data, that is related to the main relaxation process via the free volume mechanism but a smaller portion, $V_f - \Delta V$. In this context it is physically reasonable to assume that the lower wing of the hole size distribution contains holes too small to show a liquid-like behaviour and an activation energy is required for the cooperative rearrangement of molecules. Larger holes may, however, show this behaviour and allow a free exchange of free volume in their surroundings by thermal fluctuations, i.e. without a thermal activation in the ordinary sense.

It is now interesting to find out whether ΔV, which quantifies the deviation of the relaxation data from the original CT model, shows some correlation with other material properties. For polymers, for example, some of us found that ΔV correlates to the difference between the Vogel temperature T_0 from relaxation experiments and T_0' derived from the linear extrapolation of the free volume down to zero (equations (5)), $\Delta V = E_f(T_0 - T_0')$, and that it rises linearly with T_g: ΔV (cm^3 g^{-1}) $= -0.100(\pm0.02) + 4.3(\pm0.6) \times 10^{-4} T_g$ (K) [42]. These results show that high-T_g polymers need a large hole free volume to pass into the liquid (or rubbery) state and that this required hole volume grows with T_g faster than the mean hole free volume $V_f(T_g)$. This causes the increase in the difference between T_0 and T_0' and in the value of ΔV with T_g. A variation of $\Delta V = 0.015$–

0.06 $cm^3\ g^{-1}$ and $T_0' = T_0 - (20–75)$ K was estimated [42]. An almost perfect agreement with the CT theory, $\Delta V = 0$ and $T_0' = T_0$, was observed for polymers with very low T_g, such as polyisobutylene (PIB) [43] and polymethylphenylsiloxane (PMPS) [44].

In this context it is interesting that a similar result to the described behaviour of ΔV is found when applying the configurational entropy approach of Adam and Gibbs [45] to the glass transition of polymers. This theory describes the α relaxation frequency by the Adam–Gibbs equation $\log_{10}\omega = \log_{10}\omega_0 - (C_{AG}/\ln 10)/TS_c$, where S_c is the configurational entropy and C_{AG} is a constant. Cangialosi *et al* [46] found that a residual excess entropy S_{ex} exists for high T_g polymers at the Vogel temperature T_0 and concluded that the Adam–Gibbs equation remains valid when the contribution of the secondary (β) relaxation process uncoupled to the α process to the configurational entropy is taken into account, $\log_{10}\omega = \log_{10}\omega_0 - (C_{AG}/\ln 10)/TS_{ex,\alpha}$, where $S_{ex,\alpha} = S_{ex} - S_{ex,\beta}$. This contribution, $S_{ex,\beta}$, turns out to be essentially temperature-independent. This result stimulates the interesting idea that the volume correction term ΔV may have some connection to the β relaxation process. The volumetric activity of the β process is not yet systematically investigated. In general it is assumed that it is zero or very small due to its local nature. We remark, however, that in the case of poly(methyl methacrylate) (PMMA, i.e. the polymer with the largest value of $\Delta V = 0.062$ $cm^3\ g^{-1}$ [42]) three linear ranges of thermal expansion of the *o*-Ps lifetime were observed with interception points of 355 K (T_g) and 251 K [47]. The latter temperature agrees with the secondary transition temperature T_β.

Plots of $[d\log_{10}\omega/dV_f]^{-1/2}$ versus V_f show, like the Stickel graphics, two linear ranges with the transition at a V_f corresponding to T_B. Corresponding fits of the relaxation frequency in the temperature ranges $T_g < T < T_B$ and $T_B < T < T_{kv}$ (top part of figures 8 and 9) give the parameters $\log_{10} C$, γV_f^* and ΔV.

The results of all of these plots (VFT equation (8), CT equation (9) and CG equation (6)) for the samples under study in our projects are displayed in table 3. The materials are arranged with respect to increasing T_g. We attempt to find some tendencies in the behaviour of the relaxation and free volume parameters for the different glass formers as a function of T_g or of the fragility of the material defined as $m = [d(\log_{10}\tau)/d(T_g/T)]_{T_g}$ ($\tau = 1/\omega$). We observe that the van der Waals liquids Salol, BMPC, BMMPC and PDE show $T_0^{CG} \approx T_B > T_g$ while for the ionic liquid Verapamil hydrochloride $T_0^{CG} \approx T_g$. For the latter material a single VFT function can describe the relaxation data in the whole temperature range above the experimentally investigated T_g. We may speculate that $T_B \approx T_g$, but there seems to be no correlation between T_0^{CG} and $T_0'^{CG}$, the CG temperature from the free volume fit. For Salol and PDE $T_0'^{CG} < T_0^{CG}$ is observed while for BMPC and BMMPC this relation inverts, and for Verapamil hydrochloride $T_0'^{CG} \approx T_0'^{CG}$. It seems that further research is required to interpret this behaviour.

For most of the samples we observed a good correlation of the parameters from VFT and CT fits in the temperature range $T > T_B$. We found $\log_{10}\omega_0 = \log_{10} C$ within the error limits of the data for all materials, with the exception of BMPC. Small values of the VFT constant B correlate well with low values of γV_f^*. Only for Verapamil hydrochloride is a rather large B, however correctly associated with a large γV_f^*, observed. The Vogel temperature T_0 (derived for $T > T_B$) appears below or near T_g. For all samples, except BMPC, we have $T_0 > T_0'$, the temperature where the linearly extrapolated free volume goes to zero. For these samples we can confirm also the relation $\Delta V(\text{CT fit}) = \Delta V_{calc} = E_f(T_0 - T_0')$ ($E_f = dV_f/dT$). Reasons for this behaviour are discussed in detail in previous works [24, 25]. For BMPC we found $T_0 < T_0'$, consequently followed by a negative value of ΔV_{calc}, which is in disagreement with ΔV obtained from the CT fit. The reason for this discrepancy is not yet clear to us. The deviation of some parameters of Verapamil hydrochloride from those for the other materials can be attributed to the ionic nature of this material. The ΔV values vary between 0.001 and 0.0034, other than the polymers, as no clear correlation of ΔV with T_g (or with the fragility m) can be observed. Obviously, we have to collect more experimental information to clarify this question.

CT fits in the temperature range $T_g < T < T_B$ deliver ΔV values between 0.0002 and 0.0035 $cm^3\ g^{-1}$ (in the case of Salol -0.01 $cm^3\ g^{-1}$, table 3). These small values agree with results for DGEBA monomers [24] and for polymers with low T_g (PIB [43] and PMPS [44]), where $\Delta V \approx 0$, i.e. the validity of the CT theory, was found. We made no fits for BMPC and BMMPC since in the limited temperature range $T_g < T < T_B$ the accuracy of the free volume is not high enough to do so. We also would like to remark that the relaxation data from this temperature range do not show a strict VFT behaviour [39–41]. The meaning of the VFT and CT fitting parameters is therefore not clear (as indicated by the large unphysical values of $\log_{10}\omega_0$, for example). The small values of ΔV may, however, show the change in the character of the dynamics at T_B and a transition to a more CT-like behaviour below T_B.

The *o*-Ps lifetime of various low-molecular-weight glass formers was studied by Ngai *et al* and correlated to relaxation and mean square atomic displacement data [15]. These authors found that fragile systems such as ortho-terphenyl (OTP) and propylene carbonate (PC) have larger hole sizes and more pronounced (sharp) thermal transitions than stronger glasses like glycerol and propylene glycol (PG) and estimated $T_{k\tau 3}/T_g \approx 1.2$ for fragile and $T_{k\tau 3}/T_g \approx 1.5$ for strong systems (the knee temperature $T_{k\tau 3}$ was denoted by these authors by T_r). Moreover, it was concluded that $T_{k\tau 3} \approx T_B$. For testing whether our samples follow this rule we have plotted in figure 10 the mean, $\tau_3 = \langle\tau_3\rangle$, and the standard deviation, σ_3, of the *o*-Ps lifetime distribution for the four materials under discussion. For comparison we involved here the data for DGEBA monomers from a former work of one of us [24] and the data for glycerol published by Bartoš *et al* [10]. The latter data come from the discrete term fits and a value for σ_3 is unavailable.

As the figure shows glycerol, which has a small fragility of $m = 49$, exhibits small hole sizes (τ_3 varies between 0.9 and 2.1 ns) and soft thermal transitions with $T_{b1}/T_g^{PALS} = 1.3$ and $T_{k\tau 3}/T_g^{PALS} = 1.5$. DGEBA has the highest fragility

of $m = 98$. τ_3 varies between 1.3 and 2.6 ns and shows distinctly sharper thermal transitions. Between T_g and $T_{k\tau 3} = 1.28T_g^{PALS}$ the *o*-Ps lifetime varies linearly without any bend, which could be used to estimate a T_{b1}. All other samples, where fragility varies between $m = 62$ and 87 (table 3), show a similar variation of the *o*-Ps lifetime with $T_{k\tau 3}/T_g^{PALS}$ values between 1.21 (PDE) and 1.38 (BMPC). PDE, Salol and Verapamil hydrochloride ($m = 75$, 80 and 87) show sharp thermal transitions without any indication of a T_{b1}. The transition around T_g is rather soft for BMPC ($m = 66$) and BMMPC ($m = 62$) and a temperature T_{b1} can be estimated when decomposing the curve into linear parts (see figures 3 and 4 and table 1).

Recently, Bartoš *et al* [13] speculated that the transition in τ_3 at T_{b1} can be ascribed to transitions from an α relaxation (primary relaxation, $T > T_{b1}$) dominated to an 'excess wing' (secondary relaxation, $T_g < T < T_{b1}$) dominated dynamics. The disappearance of the latter regime in fragile liquids was attributed to the rapid decrease in the α relaxation times with decreasing T in these materials and that the excess wing dominated region of the relaxation behaviour is reached rather close to T_g, which makes T_{b1} hardly to be separated from T_g. The T_B/T_g values of the fragile materials vary between 1.11 and 1.26 and show no distinct correlation with $T_{k\tau 3}/T_g^{PALS}$. All these values are, however, smaller than for glycerol, where $T_{k\tau 3}/T_g^{PALS} \approx T_B/T_g^{\tau} \approx 1.5$.

Novikov *et al* [48] theorized that fragile systems have an even narrow distribution of hole sizes in comparison to strong glasses. The analysis of our lifetime spectra with the routine LT9.0 allows us to estimate the width of the *o*-Ps distribution attributed to the hole size distribution. Figure 10 shows that, in agreement with this hypothesis, the fragile glass formers DGEBA and VH have rather small distribution widths σ_3. However, the larger differences in σ_3 for BMPC and BMMPC and the rather large values for Salol cannot be understood only with the concept of fragility.

Obviously, for larger differences in the fragility, the positron lifetime mirrors the dynamic character of the glass former. For smaller differences, additional effects like the character of bonds and chemical structure of the material may affect the magnitude, distribution and thermal transition of glass formers.

4. Conclusion

In this work, the local free volumes of two van der Waals liquids, BMPC and BMMPC, were investigated as a function of temperature by PALS. The results are compared to those for other more fragile or less fragile small-molecule liquids. The mean and the standard deviation of the *o*-Ps lifetime distribution, $\tau_3 = \langle\tau_3\rangle$ and σ_3, and the corresponding parameters of the volume distribution ($\langle v_h\rangle$ and σ_h) of subnanometer size holes where *o*-Ps is localized and annihilated show a typical glass transition behaviour with a weak linear expansion below T_g and a strong expansion above that temperature. In the case of BMPC and BMMPC the transition around T_g is rather flat and allows the estimation of an intermediate temperature T_{b1}, $T_g < T_{b1} < T_{k\tau 3}$, from a straight line approximation. Such a behaviour was observed (more pronounced) in the past for strong liquids like glycerol but not for fragile liquids like PDE, Salol and Verapamil hydrochloride, which show a single sharp transition at T_g. At a higher temperature, denoted as a 'knee' temperature $T_{k\tau 3}$, the *o*-Ps lifetime τ_3 shows a levelling off, which was attributed to the small relaxation time of primary (α) relaxation, $\tau_\alpha \leqslant \tau_3$. The ratio $T_{k\tau 3}/T_g$ amounts to 1.3–1.4 for BMPC and BMMPC. For fragile and strong liquids the ratios of $T_{k\tau 3}/T_g$ of 1.2–1.3 and ~1.5, respectively, were observed.

From plots of the macroscopic volume V versus the hole volume $\langle v_h\rangle$ the number density of holes is estimated to be (0.3–0.4) $\times 10^{21}$ g^{-1}, corresponding to 0.4–0.5 nm^{-3} at room temperature. The estimated specific free volume V_f varies between 0.015 at 100 K to 0.07 and 0.08 at 350 K. For T_g values V_f of 0.022 cm^3 g^{-1} (BMPC) and 0.021 cm^3 g^{-1} (BMMPC) were estimated.

The experimentally determined free volume is used to test the primary (α) dielectric relaxation data with respect to the validity of various free volume models. We found that the extended free volume theory of Cohen and Grest can be fitted to this free volume and to the dielectric relaxation data, but the parameters of both fits do not seem to be completely consistent. The classical Cohen–Turnbull free volume theory describes the structural dynamics only after introducing a corrected free volume ($V_f - \Delta V$), where ΔV was estimated to be 0.0126 cm^3 g^{-1} (BMPC) and 0.0169 cm^3 g^{-1} (BMMPC). It is concluded that it is not the entire specific hole free volume V_f, as calculated from the PALS data, which is related to the main relaxation process via the free volume mechanism, but a smaller portion. Small holes may not show a liquid-like behaviour in their surroundings, but larger holes may do so. No clear correlation of ΔV with T_g (as found for polymers) or the fragility m could be observed in the case of the glass formers studied here. We concluded that, for large differences in the fragility of different glass formers, the positron lifetime may mirror the different character of these materials. For small differences in the fragility, additional properties like the character of bonds and the chemical structure of the material may affect the size, distribution and thermal behaviour of the free volume.

Acknowledgments

The authors wish to thank J Bartoš, Bratislava, for supplying the data for glycerol and for stimulating discussions on the subject. J Kansy, Katowice, is acknowledged for delivering the analysing routine LT9.0.

References

[1] Cohen M H and Turnbull D 1959 *J. Chem. Phys.* **31** 1164
Turnbull D and Cohen M H 1970 *J. Chem. Phys.* **52** 3038
[2] Grest G S and Cohen M H 1981 *Adv. Chem. Phys.* **48** 455
[3] Bendler J T, Fontanella J J, Shlesinger M F, Bartoš J, Šauša O and Krištiak J 2005 *Phys. Rev.* E **71** 031508
[4] Tanaka H 2005 *J. Non-Cryst. Solids* **351** 3385
[5] Paluch M, Roland C M, Casalini R, Meier G and Patkovski A 2003 *J. Chem. Phys.* **118** 4578

[6] Pethrick R A 1997 *Prog. Polym. Sci.* **22** 1
[7] Jean Y C, Mallon P E and Schrader D M (ed) 2003 *Principles and Application of Positron and Positronium Chemistry* (Singapore: World Scientific)
[8] Hensel-Bielowka S, Ziolo J, Paluch M and Roland C M 2002 *J. Chem. Phys.* **117** 2317
[9] Casalini R, Paluch M and Roland C M 2003 *Phys. Rev.* E **67** 031505
[10] Bartoš J, Šauša O, Krištiak J, Blochowicz T and Rössler E 2001 *J. Phys.: Condens. Matter* **13** 11473
[11] Bartoš J, Šauša O, Račko D, Krištiak J and Fontanella J J 2005 *J. Non-Cryst. Solids* **351** 2599
[12] Bartoš J, Alegría A, Šauša O, Tyagi M, Gómez D, Krištiak J and Colmenero J 2007 *Phys. Rev.* E **76** 031503
[13] Bartoš J, Majernik V, Iskrová M, Šauša O, Krištiak J, Lunkenheimer P and Loidl A 2010 *J. Non-Cryst. Solids* **356** 794
[14] Vass S, Patowski A, Fischer E W, Süvegh K and Vertes A 1999 *Europhys. Lett.* **46** 815
[15] Ngai K L, Bao L R, Yee A F and Soles C L 2001 *Phys. Rev. Lett.* **87** 215901
[16] Dlubek G, Shaikh M Q, Raetzke K, Faupel F and Paluch M 2008 *Phys. Rev.* E **78** 051505
[17] Dlubek G, Shaikh M Q, Raetzke K, Faupel F, Pionteck J and Paluch M 2009 *J. Chem. Phys.* **130** 144906
[18] Dlubek G, Shaikh M Q, Rätzke K, Pionteck J, Paluch M and Faupel F 2010 *Eur. J. Pharmaceut. Sci.* submitted
[19] Kansy J 2008 *Acta Phys. Pol.* A **113** 1397
[20] Dlubek G, Stejny J and Alam M A 1998 *Macromolecules* **31** 4574
[21] Dlubek G, Pionteck J and Kilburn D 2004 *Macromol. Chem. Phys.* **205** 500
Dlubek G, Bondarenko V, Al-Qaradawi I Y, Kilburn D and Krause-Rehberg R 2004 *Macromol. Chem. Phys.* **205** 512
[22] Gerharz B, Meier G and Fischer E W 1990 *J. Chem. Phys.* **92** 7110
[23] Meier G, Gerharz B, Boese D and Fischer E W 1991 *J. Chem. Phys.* **94** 3050
[24] Dlubek G, Hassan E M, Pionteck J and Krause-Rehberg R 2006 *Phys. Rev.* E **73** 0318031
[25] Dlubek G, Pionteck J, Shaikh M Q, Hassan E M and Krause-Rehberg R 2007 *Phys. Rev.* E **75** 021802
[26] Dlubek G 2006 *J. Non-Cryst. Solids* **352** 2869
[27] Tao S J 1972 *J. Chem. Phys.* **56** 5499
[28] Eldrup M, Lightbody D and Sherwood J N 1981 *Chem. Phys.* **63** 51
[29] Stepanov S V, Mikhin K V, Zvezhiskii D S and Byakov V M 2007 *Radiat. Phys. Chem.* **76** 275
[30] Zoller P and Walsh C J 1995 *Standard Pressure–Volume–Temperature Data for Polymers* (Lancaster, Basel: Technomic Publ)
[31] Dlubek G, Sen Gupta A, Pionteck J, Krause-Rehberg R, Kaspar H and Lochhaas K H 2004 *Macromolecules* **37** 6606
[32] Kilburn D, Dlubek G, Pionteck J, Bamford D and Alam M A 2005 *Polymer* **46** 859
Kilburn D, Dlubek G, Pionteck J, Bamford D and Alam M A 2005 *Polymer* **46** 869
[33] Paluch M, Casalini R and Roland C M 2003 *Phys. Rev.* E **67** 021508
[34] Corezzi S, Capaccioli S, Casalini R, Fioretto D, Paluch M and Rolla P A 2000 *Chem. Phys. Lett.* **320** 113
[35] Sillescu H 1999 *J. Non-Cryst. Solids* **243** 81
[36] Donth E 2001 *The Glass Transition: Relaxation Dynamics in Liquids and Disordered Materials* (Berlin: Springer)
[37] Ngai K L 2000 *J. Non-Cryst. Solids* **275** 7
[38] Ngai K L 2003 *J. Phys.: Condens. Matter* **15** S1107
[39] Stickel F 1995 *PhD Thesis* Mainz University, Germany (Aachen: Shaker)
[40] Stickel F, Fischer E W and Richert R 1996 *J. Chem. Phys.* **104** 2043
[41] Hansen C, Stickel F, Berger T, Richert R and Fischer E W 1997 *J. Chem. Phys.* **107** 1086
[42] Dlubek G 2010 *Polymer Physics: From Suspensions to Nanocomposites to Beyond* ed L A Utracki and A M Jamieson (Hoboken, NJ: Wiley)
[43] Kilburn D, Wawryszczuk J, Dlubek G, Pionteck J, Häßler R and Alam M A 2006 *Macromol. Chem. Phys.* **207** 721
[44] Dlubek G, Shaikh M Q, Krause-Rehberg R and Paluch M 2007 *J. Chem. Phys.* **126** 024906
[45] Adam G and Gibbs J II 1961 *J. Chem. Phys.* **34** 120
[46] Cangialosi D, Alegría A and Colmenero J 2005 *Europhys. Lett.* **70** 614
[47] Wang C L, Hirade T, Maurer F H J, Eldrup M and Pedersen N J 1998 *J. Chem. Phys.* **108** 4654
[48] Novikov V N, Sokolov A P, Strube B and Surovtsev N V 1997 *J. Chem. Phys.* **107** 1057